UCRL - 75826 Rev. 1
PREPRINT

Conf-741017--35

LAWRENCE LIVERMORE LABORATORY
University of California/Livermore, California

A MODULARIZED MIRROR FUSION REACTOR CONCEPT WITH EMPHASIS ON FABRICABILITY, ASSEMBLY, AND DISASSEMBLY*

M. A. Peterson, R. W. Werner
M. A. Hoffman and G. A. Carlson

Revised May 1, 1975

This Paper was Originally Prepared for Presentation at the American Nuclear Society Winter Meeting Washington, D. C. - October 27-31, 1974

UCRL-75826 Rev. 1

A MODULARIZED MIRROR FUSION REACTOR CONCEPT WITH EMPHASIS ON FABRICABILITY, ASSEMBLY, AND DISASSEMBLY*

M. A. Peterson, R. W. Werner
M. A. Hoffman and G. A. Carlson
Lawrence Livermore Laboratory

ABSTRACT

This paper is a progress report on a continuing study directed toward the development of mirror reactor designs which simultaneously satisfy the various engineering, economic, and maintenance considerations. Two new blanket and coil structure designs are presented which satisfy engineering requirements equally as well as previous designs while offering substantial gains in accessibility for maintenance. Because of the commercial requirement for a high duty cycle and the possible high frequency of blanket module removal--for either maintenance or replacement--the module removal must be accomplished quickly with a minimum disruption of reactor operations. The blanket and coil structure

* Work performed under the auspices of the United States Energy Research & Development Administration.

designs presented in this paper allow the removal of any one of the identical blanket modules without disturbing either the remaining modules or the coil and its associated support structure. With fabricated coil structure costs estimated at $2.50/lbm and the reactor net electrical power calculated from a plasma and reactor system model detailed in the paper, coil and support structure costs of between 100-200 $/kwe were estimated.

Revision 1

A MODULARIZED MIRROR FUSION REACTOR CONCEPT WITH EMPHASIS ON FABRICABILITY, ASSEMBLY, AND DISASSEMBLY

M. A. Peterson, R. W. Werner
M. A. Hoffman and G. A. Carlson

Lawrence Livermore Laboratory

I. INTRODUCTION

Recent conceptual design studies of all three classes of magnetic containment fusion reactors have made it evident that in addition to the importance of developing a consistent set of containment physics and nuclear engineering data--the energy flow aspects of a reactor--it is equally important to include in reactor design such practical considerations as how it is put together, taken apart, and serviced as required. In mirror fusion reactors the integrated design of a viable blanket and coil support structure within the severe constraints imposed by topological, structural, economic, and maintenance considerations is one of the most difficult mirror reactor design challenges. Structural support of the mirror coils is difficult because of the extremely large forces involved (typically a total force of about 1×10^{11} Newtons at a mirror field strength of 20T), and the complex field topology imposed by the confinement physics. In addition to supporting these enormous magnetic forces a viable coil structure design must also successfully interface with the blanket module geometry. The blanket modules must be easily accessible for inspection, repair, and replacement.

Of course, in addition to the above, the economic feasibility of a blanket and coil structural configuration must also be established.

This paper is a progress report on one aspect of a continuing study directed toward the analysis of a mirror reactor design which simultaneously satisfies the requirements of the various engineering, economic, and maintenance considerations. While the blanket/coil structure proposed in previous mirror reactor studies may have potentially satisfied engineering requirements, its maintainability was very marginal.

II. REFERENCE DESIGN BASIS

The design basis of this study is a D-T fueled mirror fusion reactor with a superconducting "Yin Yang" geometry magnet with a fixed coil radius of 10 meters (Figure 1). The reactor is fueled by neutral injection. The fusion neutron energy is converted into thermal energy and tritium is produced in a modular blanket surrounding the plasma. The plasma and reactor power balances were evaluated from the analytical model detailed in Appendix A. The reactor injection energy was fixed at 200 keV. The value of $Q = 1.2$ for the chosen injection energy and vacuum mirror ratio ($R_{vac} = 3.0$) was determined from past Fokker-Planck calculations. With the selected value of $\beta = .70$ and the fixed plasma volume, the total fusion power generated was determined as a function of the mirror field strength. The reactor net electrical power was then calculated by combining the total fusion power and selected representative values of the system component efficiencies in an energy flow model of the reactor system

(Appendix A). The reactor net electrical power was used to evaluate the economic merit of each coil structure design in terms of dollars per kilowatt of net electrical power for a given mirror flux density. A summary of the reactor and plasma parameters utilized in this study is given in Table 1.

The energy of about 80% of charged particles escaping through the mirror region is directly converted into electrical energy. Selective leakage[1] of the charged particles through a local minimum in the mirror field is required to reduce the size of the magnetic expander for the direct converter, and also because it appears that an economically viable coil structure at the required field strengths will inevitably block off some of the mirror region. While the majority of the charged particle energy is directly converted into electrical energy, the small fraction[1] ($\lesssim$ 20%) of the charged particles which are not successfully selectively leaked into the direct converter must be thermally converted in the mirror region. A previous study of reactor first wall cooling under high charged particle fluxes indicates that thermal conversion of the anticipated non-selectively leaked charged particle flux $\left(\approx 200 \frac{\text{watt}}{\text{cm}^2}\right)$ can be accomplished with a simple convectively cooled tube wall.[2] Both baffling and pumping will be utilized to reduce back-streaming of the thermally converted and neutralized charged particles into the central plasma volume. Since the fraction of the total 4π solid angle subtended by these charged particle thermal converters is non-negligible ($\approx$ 5%), additional canned lithium may be required behind the thermal converter tube wall to maintain an adequate tritium breeding ratio.

III. THE BLANKET MODULE

Although there are significant differences in the detailed blanket configuration of each of the reactor designs discussed in this report, the basic module geometry is similar. The blanket is constructed of wedge-shaped modules which are assembled into two principal units whose topology approximates the "Yin Yang" field geometry (Figure 2). With the exception of the four small turn-around modules, all the other modules may be identical and the size of the blanket modules (for a given coil size) may be varied over a considerable range by varying the apex angle of the module. Although the apex angle of the blanket modules may be varied freely, the variation of module shape and thickness in the radial direction is limited both by the configuration of the coil and its supporting structure, and module removal requirements.

In this study it is assumed that as a result of the short life expectancy of blanket modules and the difficulty of insitu repair most blanket maintenance will probably require module removal from the blanket. As a result of the commercial requirement for a relatively high duty cycle and the possible high frequency of blanket module removal in early reactors (for either maintenance or replacement) module removal must be accomplished quickly with minimum disruption of reactor operations. Since there is no overlapping of blanket modules in this configuration, the possibility exists that any module might be removed without disturbing any of the other modules if sufficient clearance around the coil structure can be obtained.

Module structural rigidity may be achieved by using a portion of

the 50 to 100 cm thick radiation shield as a "strong back" support for the remainder of the blanket. Both the relatively benign environment of the shield region and the existence of potential shield materials with good structural properties seem to advocate the utilization of the radiation shield for structural support.

In this study primary attention will be focused upon helium coolant with stationary lithium for tritium breeding. However, limited preliminary work suggests that the use of liquid lithium as a coolant is perhaps possible as a result of the similar topology between the blanket geometry and the field geometry.

IV. THE COIL SUPPORT STRUCTURE

While the coil support structure is an important facet of reactor design for any magnetic confinement machine, it presents particularly severe problems in mirror machines. Even without consideration of blanket access requirements, the coil support structural problem is quite formidable. The most prominent aspect of the coil structure is simply the immense magnitude of the magnet force. The large magnitude of the coil forces results both from the high flux densities required in the mirror regions (12 to 20T) and the enormous size of the conductors(the coil winding is almost 7 m wide). For a magnetic field at the conductor of approximately 20T, the high field case in this report, the total primary magnetic forces attempting to spread apart the upper and lower coil windings of both mirror coils is about 1.1×10^{11} Newtons (25 billion pounds). Although there are several secondary magnetic forces,

they are not considered in this study because they are of much smaller magnitude than the primary coil forces.

In addition to the size of the magnetic forces, the structural problem is made more difficult by the complexity of the "Yin Yang" coil geometry and the substantial volume rendered inaccessible to structural members by the plasma. An additional constraint is the economic limitation upon the allowable volume of structural material. Although many different structural concepts have been investigated for this study, only two appear capable of simultaneously satisfying the constraints imposed by structural, economic, and blanket-access considerations.

V. THE FIRST DESIGN CONCEPT

In the first blanket/coil-structure design the emphasis was placed upon the blanket and module removal configuration by selecting it first and then attempting to develop a viable coil support structure. The basic wedge-shaped module geometry previously discussed was utilized in this design. The coil design has been selected to permit a constant thickness linear module profile rather than a more complex curvilinear profile (Figure 3).

Coolant manifold connections to the blanket module may be made either on the module outer (shield) surface or on the end of the module in between the mirror coils. Either location allows manifold disconnect and module removal without disturbing the external coolant manifold.

Each charged particle thermal converter and associated pumping plenum

module is located directly behind the outer end of each blanket module in the space between the upper and lower windings of the mirror coils.

Removal of blanket modules in this design is accomplished through the "mouth" of each mirror coil (Figure 3). As a result of the divergent nature of the interface between adjacent wedge-shaped blanket modules, any module may be removed without disturbing the remaining modules. Actual removal of a blanket module is effected by a simple linear, radially outward motion of the module and its associated thermal converter module along ways or rollers until it is clear of the magnet and structure. After a module is clear of the coil structure, it may be transported circumferentially around the outer perimeter of the coil structure to a containment cell. As a result of the linear module shape and removal path, neutron streaming through the gaps between adjacent modules may be prevented by forming adjacent module sides with interlocking corrugations.

Although this blanket module design is attractive from the blanket point of view, it imposes severe constraints upon the coil support structure. The primary repulsive magnetic force between the upper and lower mirror coil windings is contained by a set of wedge-shaped "C" clamp structures evenly spaced around the outer perimeter of both mirror coils (Figure 4). Each "C" clamp is centered on the radial dividing line between adjacent modules. The cross-sectional configuration of the "C" clamp throat (as defined on Figure 4A) must be shaped so that sufficient open space between clamps exists to allow each module to be removed through the mirror mouth between adjacent "C" clamps. This wedge shaped cross-section imposed by blanket module

removal requirements greatly increases the volume of structural material required to contain a given magnetic force. Local bending of the coil windings between adjacent "C" clamps is limited by a plate beam on the upper coil surface. Two different "C" clamp structural configurations were developed to investigate the first order economic and structural feasibility of "C" clamp magnet supports.

Initially, a simple solid wedge-shaped "C" clamp carrying the majority of the load in bending was utilized to balance the opposing upper and lower coil winding forces (Figure 4A). The wedge shape of the "C" clamp throat was determined from the previously mentioned cross sectional constraint imposed by blanket module removal requirements. The width of the "C" clamp throat in the radial direction ("w"; Figure 4a) was selected to yield a maximum stress of 10^5 psi. For this preliminary analysis, the maximum stress in the "C" clamp throat was calculated by treating the throat cross section as a beam subjected to the combined moment and tension loading due to the resultant of the magnetic force (Appendix B). This preliminary structural analysis indicated that solid wedge-shaped "C" clamps could contain magnetic forces resulting from fields of up to 20T with a maximum design stress of 10^5 psi. Although the solid wedge-shaped "C" clamp appears capable of restraining the magnetic forces, its structural efficiency is poor, because the cross sectional shape dictated by module removal requirements has poor structural properties. In calculating the structural volume of a solid wedge-shaped "C" clamp structural support system, it was assumed that the cross sectional area of structural material throughout the "C" clamp would be equal

to the cross section required at the "C" clamp throat. An allowance was also added for the plate beam used to restrain coil bending between "C" clamps. With the above assumptions, a structural volume for the high field case ($B_{cond.} \approx$ 20T. of about 21,800 m^3 was calculated. Based upon superconductor costs from a previous study[3], a fabricated coil structure cost of 2.5 \$/lb., and the reactor model from Appendix A, an estimated total coil and structure cost of 517 \$/Kwe was obtained. Thus, while the wedge shaped "C" clamp design appears capable of satisfying structural and accessibility requirements, its economic viability appears doubtful.

Because the reactor fusion power ($\propto B^4$; Appendix A) falls faster with decreasing field strength than the magnet and structure costs ($\propto B^2$), the cost of the magnet and structure relative to the reactor net electrical power rises as the magnetic field strength is lowered.

An alternate, structurally more efficient "C" clamp model was developed to provide an indication of the reduction in structural volume that might be achievable within the severe constraints imposed by this blanket module removal concept (Figure 4b). In contrast to the previous "C" clamp design which carried most of the magnetic force in bending, this second "C" clamp model is a simple pin-jointed frame or truss which ideally carries all loads in tension or compression. This alternate "C" clamp model consists of top and bottom horizontal "A" frames which transfer the magnet forces to vertical tension and compression members. As in the case of the previous "C" clamp structure, the cross sectional configuration of the vertical tension and compression members is partially determined by

the requirement that they fit within the wedge-shaped envelope imposed by blanket module removal requirements. The radial widths and center line locations of the vertical tension and compression members is determined by requiring that the magnitude of the stress in the two members be equal and that they be capable of supporting the magnet force resultant. The relatively short length of the compression member and the surplus of available space for an expanded cross sectional shape indicate that premature failure of the compression member by elastic instability can be avoided. The two horizontal "A" frames which transfer the magnet forces to the vertical tension and compression members were sized by the magnet force resultants and a constant design stress requirement. The much greater structural efficiency of this truss "C" clamp relative to the solid wedge "C" clamp results in a substantial reduction in the required structural volume. In favorable contrast to the solid "C" clamp structure at about 21,800 m^3, the truss "C" clamp requires a structural volume of only 8,000 m^3 for the high field case (B_{cond} = 20T). Based upon the same estimation process used previously, a coil and structure cost of about 203 \$/Kwe is indicated.

VI. THE SECOND DESIGN CONCEPT

In contrast to the approach used in developing the first design concept, the second design was begun by first selecting a potentially promising structural configuration and then developing a viable blanket and module removal configuration. Although the design process

was different, the blanket module configuration developed for the second design was in many aspects similar to the first blanket design. However, the removal method is entirely different.

The wedge-shaped module geometry is basically the same except that as a result of moving the charged particle thermal converter and associated pumping plenum into the inner half of the mirror coil gap, the module does not extend as far into the mirror region (Figure 5). Although this shortening of the blanket will probably reduce tritium breeding, it appears that because of the very low neutron flux in the mirror regions and the breeding ratio excess of previous designs ($\simeq$ 1.10 -1.20)[4] that this reduction will be tolerable. If not, then canned lithium may be placed in front of the magnet shield in the mirror region without substantially intruding into the pumping plenum area.

Module removal in this design is accomplished in the area between the opposite mirror coils rather than through the mouth of the mirror. Blanket modules are removed by first pivoting them outward about their coil end and then pulling them straight out between opposite mirror coils. After the module is clear of the blanket and upper coil turnaround, it may be transported to a containment cell. In order to allow any blanket module to be removed independently of all the others, a close fit between adjacent modules (rather than the interlocking corrugated modules sides of the first design) must be used to control neutron streaming. In contrast to the first design, this design may require removal of some of the reactor subsystems on the outer blanket surface (injectors etc.) for access to a blanket module; the first

design required removal only of the thermal converter module for access to a blanket module.

This blanket module removal design allows the coil support structure to occupy the outer one-half of the space between the upper and lower winding of each mirror coil. Basically, the coil support structure consists of a short beam which resists the tension and bending loads exerted by the magnet coil windings. The inner portion of the beam is made up of a series of tension members extending through the coil transferring their load to a coil restraining plate on the outer surface of the coil. The elements of coil conductor between the tension members piercing the coil are increased in cross sectional area to maintain the required conductor current density.

The volume fraction of tension members piercing the coil region varies from a maximum of about 90% at the surface of the coil support structure nearest the mirror point to zero at the neutral surface of the internal coil structure; the neutral surface is defined at the location where the net stress is zero. The section of the internal coil structure outside of the neutral axis transfers its compressive loading through the coil to the external coil restraining plate. The internal coil support structure and the external restraining plate are circumferentially continuous around both mirror coils with the exception of the selective leakage port(s). A pair of external "C" clamp structures may be required to contain the coil around each selective leakage port. Thus, with the exception of the selective leakage port(s), the internal coil support structure completely blocks access to the mirror region from outside of the coil.

For the purpose of a preliminary structural analysis, the distributed magnet force was replaced by an equivalent concentrated resultant force. The maximum stress in the internal coil structure was then calculated by superimposing the stress distributions resulting from the tension force and bending moment applied by the magnetic force resultant (Appendix B). This preliminary analysis indicated that magnetic fields of up to about 15T could be contained by the internal structure without exceeding a maximum stress of 10^5 psi.

A structural volume including both the internal structure and external retaining plate of about 1500 m^3 was calculated for a field strength of about 15T. In comparison, at a field strength of about 15T the solid wedge "C" clamp requires about 11,500 m^3; and the alternate truss "C" clamp requires about 4,500 m^3 (Figure 6a). Based on the model of mirror machine performance in Appendix A, a coil and a structure cost of about 139 \$/Kwe are indicated for a maximum field of 15T. By utilizing very high strength steels, modifications of the coil shape, and internal and external structural configuration changes, it may prove possible to extend this basic design configuration up to higher field levels resulting in further reductions in coil and structure costs.

For comparative purposes, the total structural volume as a function of magnetic field strength is presented in Figure 6a for all of the structural designs discussed in this paper. In Figure 6b the calculated structural volume for the various designs is combined with superconductor costs from reference 3 and the plasma and reactor system model in Appendix A to obtain the cost of the magnet and structure per kw of net electrical power as a function of the magnetic field strength.

In addition, the mass and relative cost of a structurally ideal pure tension coil support design was included for comparative purposes. While this design is impractical because it intrudes into the plasma confinement volume, it provides an absolute lower limit to the coil support structure mass required for this coil configuration.

VII. SUMMARY

The mirror reactor blanket and coil structure design configurations presented in this paper appear capable of satisfying the various reactor engineering considerations while achieving substantial gains in accessibility over previous designs. The results obtained from this study are summarized by the following remarks.

A. Preliminary structural analysis indicates that either of the external "C" clamp designs proposed for the first design concept can contain the magnetic forces resulting from mirror field strengths of 20T with a maximum design stress of $6.9 \times 10^8 \frac{N}{m^2}$ (10^5psi).

B. The truss "C" clamp structure requires only about 28% as much structural material as the solid wedge "C" clamp design. Thus, since both designs can withstand the maximum field strength, the truss "C" clamp is substantially superior to the solid wedge "C" clamp.

C. With a maximum allowable design stress of $6.9 \times 10^8 \frac{N}{m^2}$ (10^5 psi) the internal coil support structure proposed as the second design concept is restricted to field strengths of about 15T or less.

D. For field strengths below its structurally imposed limitation of 15T the internal coil support structure requires about 66% less

structural material than the external truss "C" clamp structure. Consequently, this second design concept is superior to the first.

E. The above results depend only on magnetic field strength and not on the details of the fusion plasma model or the energy flows and component efficiencies in the overall power plant.

F. For the maximum allowable field strength of 15T and with the plasm and reactor model developed in Appendix A, the coil and structure cost for the second design concept was calculated to be about 139 $/Kwe. This may be compared with a coil and structure cost for the external truss "C" clamp structure of the first design concept of 360 $/Kwe at the same field strength of 15T.

G. Although the external truss "C" clamp structural design requires considerably more structural material for the same field strength than the alternate internal coil support structure, its capability of containing higher field strengths (20T vs. 15T) with their associated higher fusion power densities results in a minimum cost of 203 $/Kwe at 20T.

APPENDIX A

SCALING OF REACTOR POWER

The bulk of this paper, concerning the design of the blanket module and the magnet structure of a mirror fusion reactor, is independent of *any* consideration of the plasma containment properties of mirror machines. However, in order to assess the relative value of coil systems of different magnetic field strength, it is necessary to consider the scaling of reactor power with magnetic field. We shall follow the methodology introduced in Ref. 3 and further developed in Ref. 5.

The axial mirror ratio in the absence of plasma is defined as

$$R_{VAC} \equiv \frac{B_m}{B_{o,vac}} ,$$

where B_m is the magnetic field strength at the mirror and $B_{o,vac}$ is the central field strength at vacuum. With plasma present, the central field is depressed to B_o, and the plasma axial mirror ratio is given by

$$R \equiv \frac{B_m}{B_o} \simeq \frac{R_{vac}}{\sqrt{1-\beta}} \qquad (A\text{-}1)$$

where β is the ratio of perpendicular (to B) plasma pressure to magnetic pressure. Specifically, β is defined by

$$\beta \equiv \frac{P_{\perp,o}}{B_{o,vac}^2/2\mu_o} = \frac{\frac{2}{3}\gamma n_{i,o} \bar{W}_i + n_{e,o} kT_e}{B_{o,vac}^2/2\mu_o}$$

where $n_{i,o}$ and $n_{e,o}$ are the central ion and electron densities ($n_{i,o} = n_{e,o}$), T_e is the temperature of the nearly Maxwellian electrons, $\bar{W}_i$ is the mean ion energy, and γ is the ion anisotropy factor. For a mirror confined plasma, the perpendicular pressure is larger than that for an isotropic Maxwellian plasma; that is, $\gamma > 1$. We shall use $\gamma = 1.27$, as did Moir in Ref. 5. We shall approximate $kT_e/\bar{W}_i = 0.1$ and $\bar{W}_i$ = the injection energy, E_{INJ}, based on the Fokker-Planck calculations reported in Ref. 6. It follows that

$$\beta = \frac{0.95\, n_{i,o} E_{INJ}}{B_{o,vac}^2/2\mu_o} \simeq \frac{n_{i,o} E_{INJ}}{B_{o,vac}^2/2\mu_o} \quad . \tag{A-2}$$

Stability requirements set a less-than-unity upper limit to the achievable value of β.

The fusion power produced by the contained plasma is given by

$$P_{FUS} = \frac{n_{i,o}^2}{4} \overline{\sigma v}_{DT} E_{FUS} \pi r_p^2 L\left(A^{2,j} C^2\right) \tag{A-3}$$

where $\overline{\sigma v}_{DT}$ is the reaction rate coefficient for the deuterium-tritium fusion reaction, E_{FUS} is the energy release per DT fusion (17.6 MeV), r_p is the radius of the plasma at the midplane, L is the distance between the mirrors, and $A^{2,j}$ and C^2 are radial and axial density

factors defined and evaluated by Moir in Ref. 3 Substituting for $n_{i,o}$ from Eq. (A-2) yields:

$$P_{FUS} = \frac{\beta^2 B_{o,vac}^4}{16\mu_o^2 E_{INJ}^2} \overline{\sigma v}_{DT} E_{FUS} \pi r_p^2 L\left(A^{2,j} C^2\right). \qquad (A-4)$$

In this study we have used a coil configuration with $R_{VAC} = 3$, $L = 20$ m, and $r_p = 4$ m (r_p is determined by the position of the last closed magnetic field contour).

We shall choose an injection energy of 200 keV (the optimum injection energy for the study reported in Ref. 2) and $\beta = 0.7$. Then from Eq. (A-1), $R = 5.5$, and from Ref. 3, $C^2 = 0.21$. We shall assume a cubic radial density profile; so $A^{2,j} = A^{2,3} = 9/20$. At a mean ion energy of 200 keV the reaction rate coefficient $\overline{\sigma v}_{DT}$ has the value 8×10^{-16} cm^3/s. Using the above values we calculate the fusion power:

$$P_{FUS}(Mw) = 4.07\left[B_{o,vac}(Tesla)\right]^4 = .0502\, B_m^4 = .0343\, B_{\substack{max \\ cond}}^4 . \qquad (A-5)$$

The last equality of Eq. (A-5) introduces the maximum field at the conductor, which we estimate to be 10% greater than the mirror field.

In order to determine the net electrical power of the reactor we must specify the elements of the mirror machine power cycle. This is done by means of a power flow diagram as discussed in Ref. 7 and shown in Fig. A-1 for the present case. The DT fusion power produced in the plasma is a factor Q times the trapped injected power. The fusion neutron power is multiplied by a factor m in the blanket and then converted to electricity by a thermal converter.

The charged particle power first passes through a direct conversion topping cycle, then through a thermal converter. Part of the gross electrical power is used to power the neutral beam injector system. The component efficiencies assumed for the present case are shown in Fig. A-1. The assumed direct conversion efficiency implies a 2 stage direct converter such as the Venetian blind type[8]. The assumed injector efficiency implies highly efficient beam direct converters for the un-neutralized portions of the beams[8,9]. The value of Q has been scaled from Fig. 4 of Ref. 7 (which was determined by the Fokker-Planck calculations reported in Ref. 6) by the scaling relation $Q \propto \log_{10} R$. It should be noted that Q reaches its maximum near $\bar{W} = 200$ keV.

The power cycle shown in Fig. A-1 has a system efficiency of 28% and a ratio of net electrical power to fusion power of 0.35.

The fusion power and net electrical power are shown in Fig. A-2 as functions of the several magnetic field strengths: $B_{o,vac}$, B_m, and B_{max} .
cond

APPENDIX B

I. GENERAL CONSIDERATIONS

In this appendix the structural models and calculational procedures used to evaluate the feasibility and structural efficiency of each coil support structure are discussed. Because of the preliminary nature of this study many simplifying assumptions were made in both the structural models and the calculational techniques used in their evaluation. Although many geometrical aspects of these coil support structures suggest that the application of numerical techniques would be necessary for accurate analysis, it is felt that the simple bending theory used in this analysis is adequate for a "preliminary" study. The coil support structures considered in this study may be naturally divided into the two catagories according to their basic geometrical configuration--"C" clamp (Figure 4a and 4b) and internal (Figure 5). The two different types of "C" clamp structures considered in this report will be discussed first.

II. "C" CLAMP STRUCTURAL DESIGNS

A. Blanket Module Removal Limitations

Because in this design concept the blanket modules are to be removed through the mirror region (Figure 3), the cross sectional shape of the throat of all "C" clamp configurations is restricted. The cross section of the throat of the "C" clamp must be within an

allowable envelope (Figure B-1). This envelope is determined by specifying a blanket module sector angle and assuming that the end of the module is located in the center of the mirror coil. Since the cross sectional shape of those regions of the "C" clamp which are clear of the blanket module removal path is not restricted, they may be freely selected to improve structural efficiency.

B. Wedge-Shaped Solid "C" Clamp Design

The throat area of the solid "C" clamp was assumed to be the critical structural region both because the bending moment is a maximum there and because module removal requirements dictate the use of a cross sectional shape with poor structural properties (small section modulus for cross sectional area). The model used for analyzing the solid "C" clamp is presented in Figure B-2. In order to evaluate the moment of inertia of the throat cross section, the following expression was developed for the location of the centroidial axis:

$$\bar{y} = \frac{w(2w + 3c)}{6(w + c)} \cdot \tag{1}$$

The moment of inertia about the centroidial axis was then obtained by integration and the parallel axis transfer theorem.

$$I = \frac{\Delta\Theta w^3}{72}\left[\frac{2w^2 + 6cw + 3c^2}{(w + c)}\right] \tag{2}$$

The maximum bending stress was then obtained from simple beam bending theory $\left(\sigma_m = \frac{Mc}{I}\right)$ and superimposed with the tension stress to yield the

maximum stress for a given design [magnetic force (F_{tot}), coil width (c), and throat width (w)].

$$\sigma_{max} = \left(\frac{2F_{tot}}{\pi c^2}\right) f(W) \tag{3}$$

$$f(W) \equiv W + \frac{(4W + 3)(4W^2 + 6W + 3)}{2W^2 + 6W + 3} \tag{4}$$

$W \equiv w/c$

It is interesting to note that this result is independent of the blanket sector angle. This is because while the load on each individual coil structure rises as the blanket sector angle increases (fewer clamps with the same total load), the cross sectional area of the clamp throat rises in such a manner as to maintain constant maximum stress. In order to estimate the volume of the wedge-shaped solid "C" clamp, it was assumed that the cross sectional area at the throat would be required throughout the "C" clamp (Figure B-3). Since the "C" clamp cross sections in regions out of the blanket module removal path can be altered to improve their structural properties (Figure B-1), this is probably a conservative estimate.

In table B-1 the maximum stress for solid "C" clamp structures of several different sizes for the high field case (B_{cond} = 20T) is presented.

C. Truss "C" Clamp Design

The structural loading in the throat tension and

compression members (Figure B-4) was determined from static equilibrium as a function of the compression and tension member geometry (r_1, r_2, t_1, t_2; Figure B-4) and the total magnetic force (F_{tot}). As in the previous solid "C" clamp design when the structural loading is expressed in terms of the total magnetic force, it is independent of the module apex angle ($\Delta\Theta$). The stress in the throat tension (σ_{1T}) and compression (σ_{2c}) members was determined by dividing their structural loading by their respective cross sectional areas as specified for a given structure geometry (r_1, r_2, t_1, t_2) by module removal requirements (Figure B-4).

$$\sigma_{1T} \frac{F_{1T}}{A_{1T}} = \frac{2F_{tot}}{\pi(t_1 + c)} t_1 \left[\frac{1}{1 - \left(\frac{t_1 + c}{2r_2}\right)}\right]$$

$$\sigma_{2c} = \frac{F_{2c}}{A_{2c}} = \frac{F_{tot}}{\pi r_2 t_2} \left[\frac{1}{\left(\frac{2r_2}{t_1 + c} - 1\right)}\right] .$$

where

$\sigma_{1T} \equiv$ the tensile stress in the throat tension member

$\sigma_{2c} \equiv$ the compressive stress in the throat compression member

$F_{tot} \equiv$ the total magnet force on one coil

c, t_1, and r_2 are defined in Figure B-4

For this analysis the geometry of the throat tension and compression members for a given total magnetic force was partially determined by requiring that the magnitude of the stress in both members be the same. By equating the two relations previously given for the stress in the throat tension and compression members, the following analytical requirement for equal stress geometries was obtained:

$$\frac{t_2}{t_1} = \frac{r_1^2}{r_2^2} \quad \text{if} \quad \sigma_{1_T} = \sigma_{2_c}$$

With a maximum allowable stress of $6.9 \times 10^8 \frac{N}{m^2}$ (10^5 psi), and the magnetic force resulting from a 20T mirror field, and the equal stress requirement the following geometry for the throat tension and compression members was selected:

$$r_1 = 5m,\ r_2 = 12m,\ t_1 = 4m,\ t_2 = .7m$$

In order to forestall elastic instabilities, the compression member cross sectional area specified by the above geometry must be redistributed about the centerline of the compression member in a tubular configuration (Figure B-4).

The "A" frame structures which transfer the magnetic forces to the throat tension and compression members were assumed to consist of pin jointed compression and tension members arranged in the statically determinate truss illustrated in Figure B-4. Since these "A" frame

structures are completely outside of the blanket module removal path, there are no restrictions on the shape of any of their tension or compression members. The forces in each of the "A" frame structural members was determined from static equilibrium considerations as a function of total magnetic force, the tension and compression member geometry, and the height of the "A" frame (h; Figure 8-4). The cross sectional area of all the "A" frame tension and compression members was then selected so that the stress in all the members was equal $\left(A_1 = F_1/\sigma_{max}\right)$. In this study no attempt was made to minimize the structural volume by optimizing the "A" frame and throat tension and compression member geometries for a given magnetic force. With the nonoptimal throat tension and compression member geometry previously selected (for $B_m = 20T$), a constant design stress in all members of $6.9 \times 10^8 \frac{N}{m^2}$ (10^5 psi) and an "A" frame height of 5 m the structural volume was calculated by summing the volume of all the tension and compression members. Since the cross sectional area of all the structural members of the truss "C" clamp scale linearly as the magnetic force, the structural volume for a fixed structural geometry (r_1, r_2, c) scales as the second power of the magnetic field strength. The total structural volume of a truss "C" clamp support system as a function of the field strength is given in Figure 6a.

III. INTERNAL COIL SUPPORT STRUCTURE

The basic geometry of the internal coil support structure is illustrated in Figure 5 and discussed in Section VI of the main body of this paper. In this preliminary analysis the distributed magnetic

force was replaced with an equivalent concentrated force acting through the center of the coil (Figure B-5). The stress distribution in the internal coil structure was calculated by superimposing the tension and bending stress distribution resulting from the bending moment and tension loading exerted by the magnetic force resultant. The bending stress was calculated from simple beam theory. The stress distribution obtained for a maximum field strength at the conductor of 15T is illustrated in Figure B-5. The magnetic force is transferred from the coil restraining plate to the internal structure through tension members which pierce the coil winding. In order to minimize the amount of conductor displaced by the tension members piercing the coil, their volume fraction (% of the coil volume) is varied proportionally with the magnitude of the stress in the internal structure. In this design the stress in all the tension members is maintained constant at the maximum allowable design stress $\left(\sigma_{max} = 6.9 \times 10^8 \frac{N}{m^2}, 10^5 \text{ psi}\right)$. Since the stress $\left(\sigma_{max}\right)$ in each of the tension members is the same and they are assumed to have the same modulus of elasticity (E), their strain $\left(\varepsilon = \frac{\sigma_{max}}{E}\right)$ must also be equal. Thus, in order to match the linear variation of displacement in the internal structure implied by simple beam theory either the tension members must be prestressed or their lengths must vary proportionally with the displacement of the internal structure. The thickness of the coil restraining plate was estimated by modeling the overhanging portion of the coil restraining plate as a cantilever beam with a uniformly distributed load. The total structural

volume of the internal structure and coil restraining plate was calculated to be approximately 1500 m^3 at its maximum allowable (stress limited) field strength of 15T. Similarly to the other coil support structures, the required structural volume scales approximately as the second power of the magnetic field strength. The variation of structural volume with magnetic field strength for the internal coil support structure is illustrated and compared with the other alternate structures in Figure 6a.

TABLE 1

I Fixed Parameters

A. Plasma Parameters (Appendix A)

$E_{fus} = 17.6$ Mev

$E_{inj} = 200$ keV

$\overline{\sigma v}_{DT} = 8 \times 10^{-16} \frac{cm^3}{sec}$

$\beta = 0.7$

$R_{vac} = 3.0$

$r_p = 4$ m

$L = 20$ m $\left(2 R_{coil}\right)$

$Q = 1.2$

B. System Parameters (Appendix A)

$\eta_{inj} = 0.90$

$m = 1.3$

$\eta_{DC} = 0.60$

$\eta_{th} = 0.45$

$$\eta_{sys} = 0.28$$

C. Coil and Structure Parameters

$R_{coil} = 10$ m

Cost of fabricated structure = \$2.50/lbm

Super conductor costs from reference 3

II. Reference Cases

A. Medium Field ($B_{cond} = 15T$)

Coil Support Structure Design	Solid "C" Clamp (Fig. 4a)	Truss "C" Clamp (Fig. 4b)	Internal Structure (Fig. 5)
(T.) $B_{cond.}$	15.	15.	15.
(T.) B_{mirror}	13.5	13.5	13.5
(T.) Bo_{vac}	4.5	4.5	4.5
(Mw) P_{fusion}	1,710.	1,710.	1,710.
(Mw) $P_{net\ electric}$	599.	599.	599.
$\left(\frac{Mw}{m^2}\right)$ Neutron Wall Loading	4.4	4.4	4.4
(m^3) Total Struct. Volume	11,500.0	4,500.0	1,500.0
$\left(\$/_{Kwe}\right)$	933.	360.	139.

B. High Field (B_{cond} = 20T)

Coil Support Structural Design	Solid "C" Clamp (Fig. 4a)	Truss "C" Clamp (Fig. 4b)	Internal Structure (Fig. 5)
(T.) B_{cond}	20.	20.	20.
(T.) B_{mirror}	18.	18.	18.
(T.) Bo_{vac}	6.	6.	6.
(Mw) P_{fusion}	5520.	5520.	5520.
(Mw) $P_{net\ electric}$	1930.	1930.	1930.
$\left(\frac{Mw}{m^2}\right)$ Neutron Wall Loading	14.1	14.1	14.1
(m^3) Total Struct. Volume	21,800.	8,400.	Not Applicable B > 15T cond
$\left(\frac{\$}{Kwe}\right)$ Coil & Struct. Cost	517.	203.	Not applicable B_{cond} >15T

TABLE B-1

Parameters

$F_{tot} = 2.67 \times 10^{10}$ N $\quad (B_{cond} \simeq 20T)$

$W \equiv w/c$ $\quad c = 6.3$ m

W	1	2	3
$\left(\frac{\text{Newton}}{m^2}\right) \sigma_{max}$	2.2×10^9	6.6×10^8	3.3×10^8
(psi) σ_{max}	3.2×10^5	9.7×10^4	4.8×10^4
$(m^3) V_{tot}$	5.14×10^3	21.6×10^3	56.7×10^3

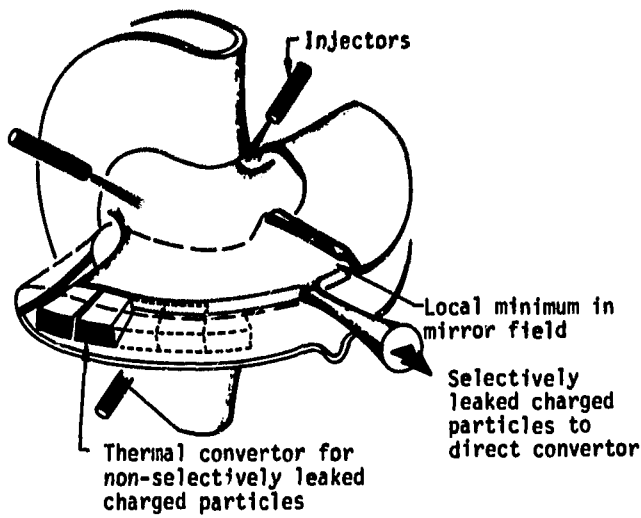

Fig. 1 General Reactor Configuration

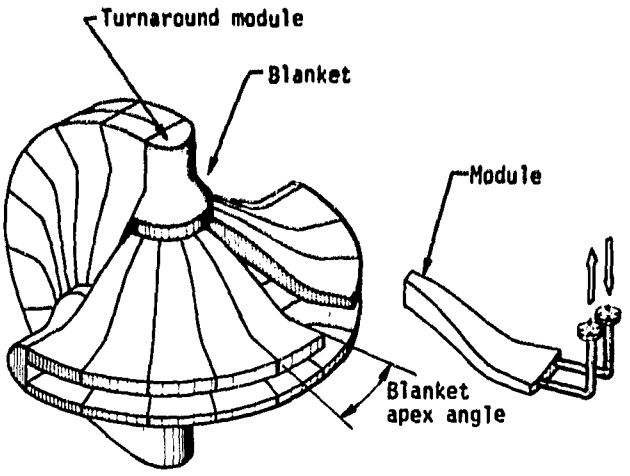

Fig. 2 General Blanket Configuration

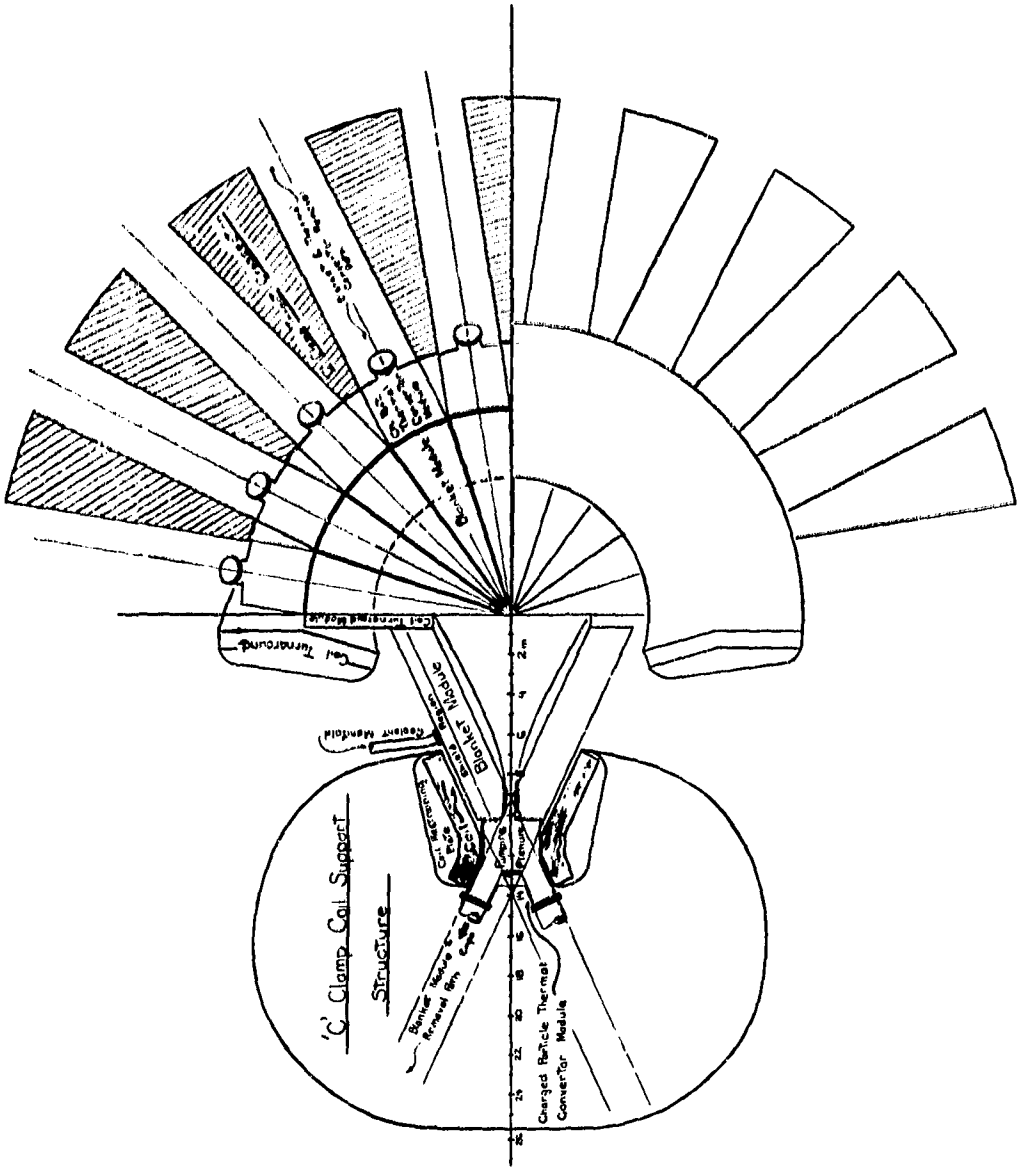

Fig. 3 Blanket and External Coil Structure Design

Figure 4a

Solid 'C' Clamp Structure

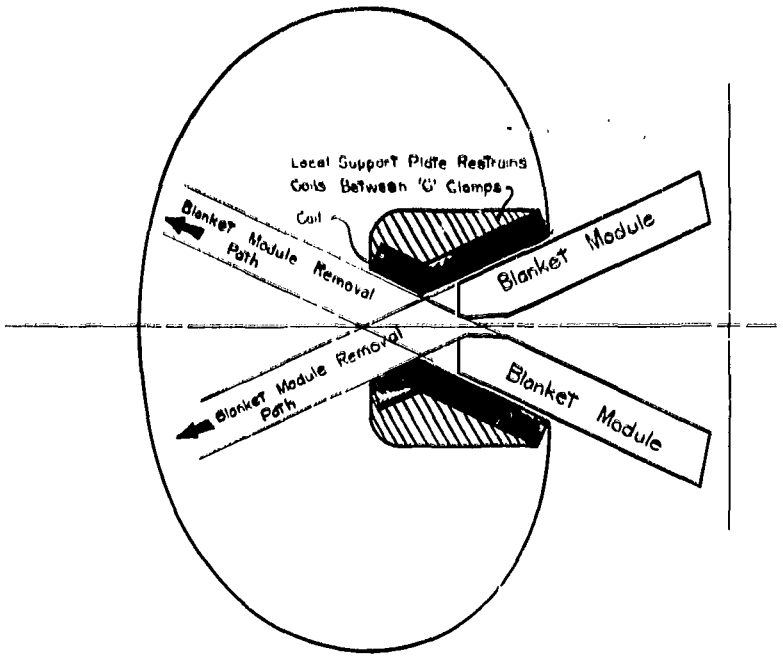

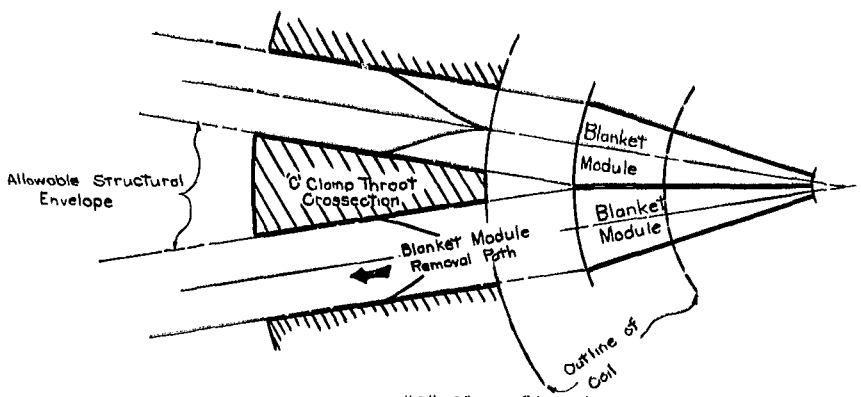

Fig. 4a Solid "C" Clamp Structure

Figure 4b

Truss 'C' Clamp Structure

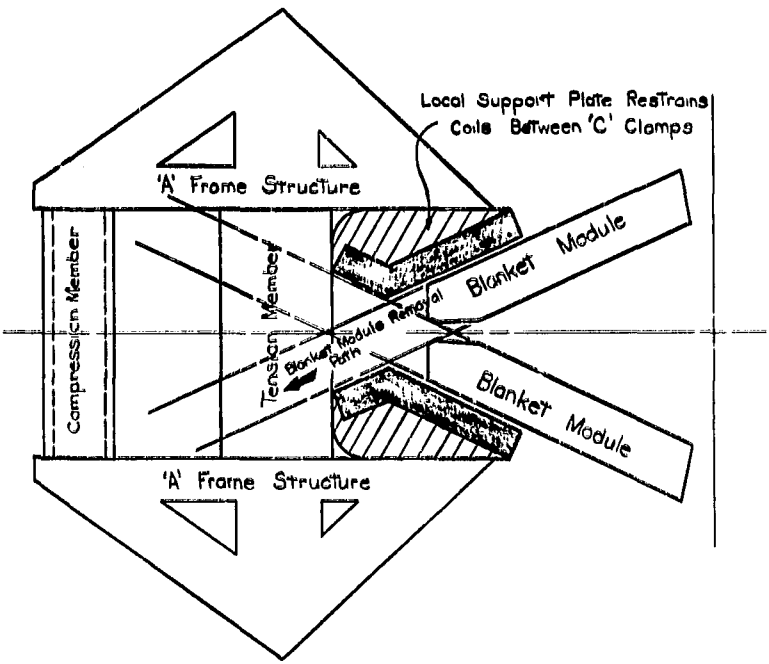

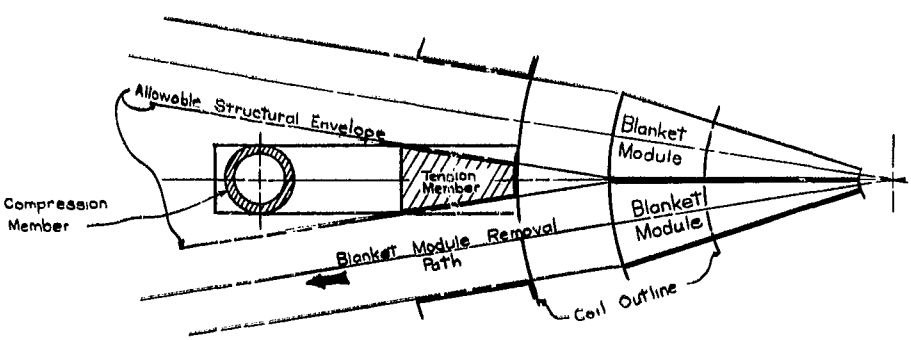

Fig. 4b Truss "C" Clamp Structure

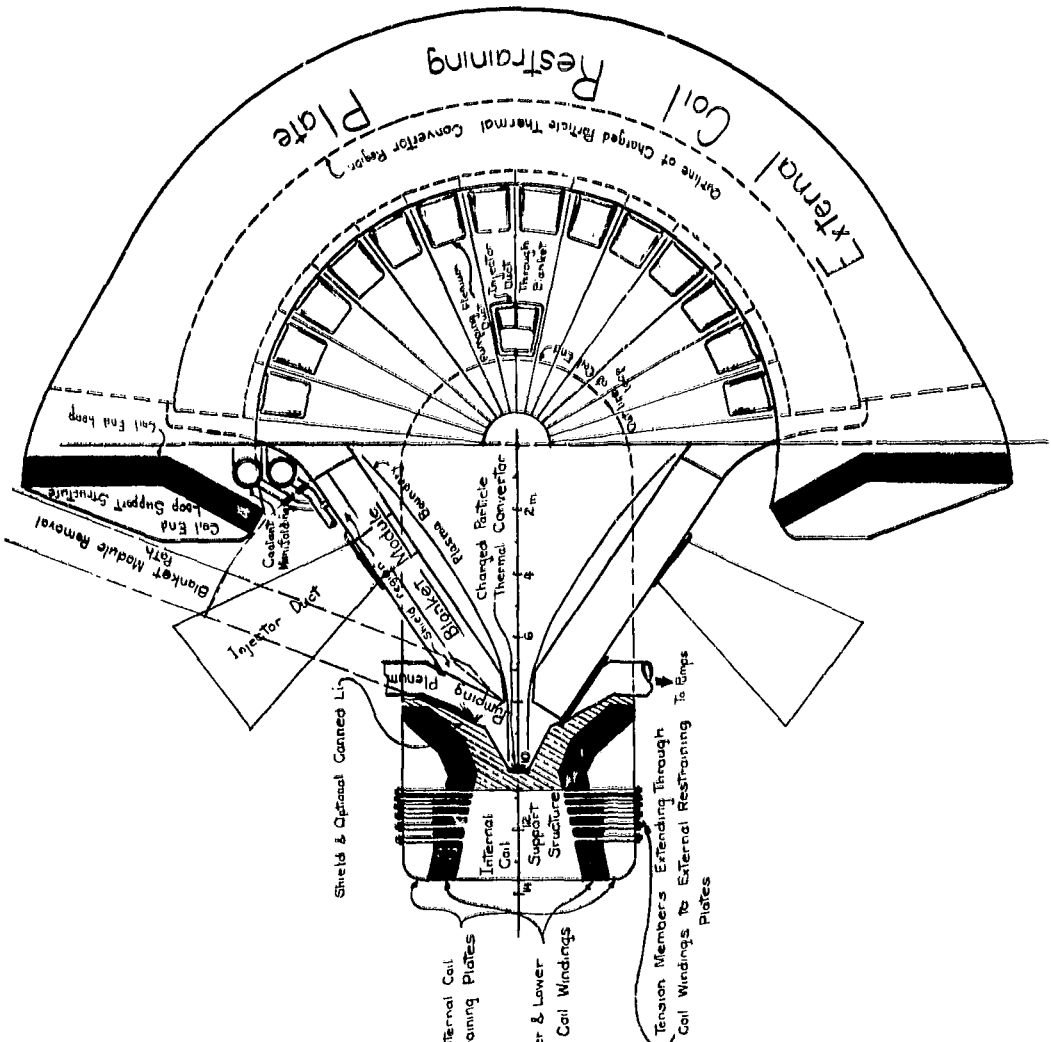

Fig. 5 Blanket and Internal Coil Structure Design

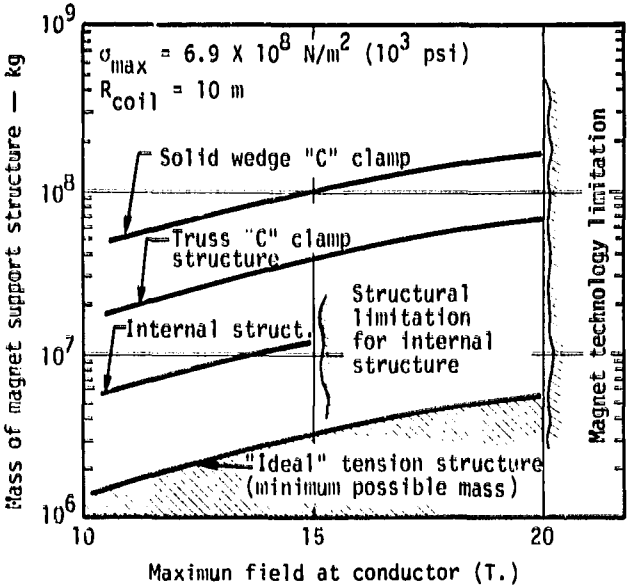

Fig. 6a Mass of Magnet Support Structures

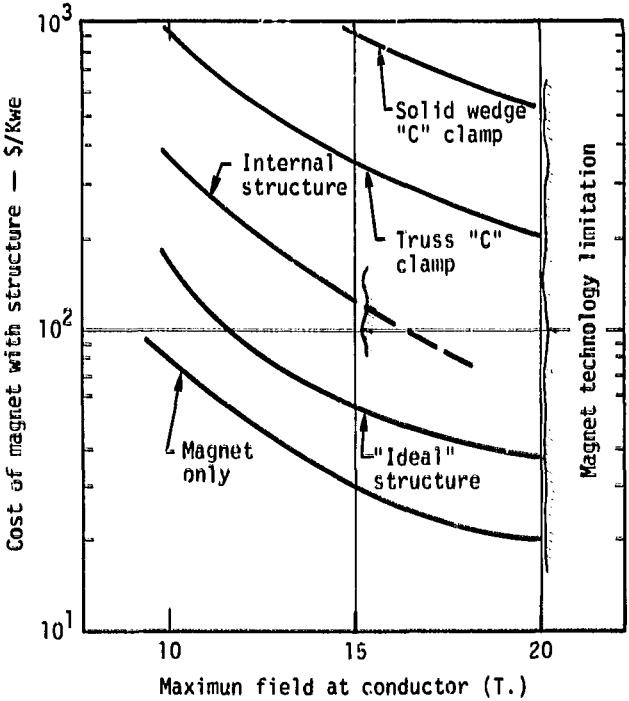

Fig. 6b Cost of Magnet with Support Structure

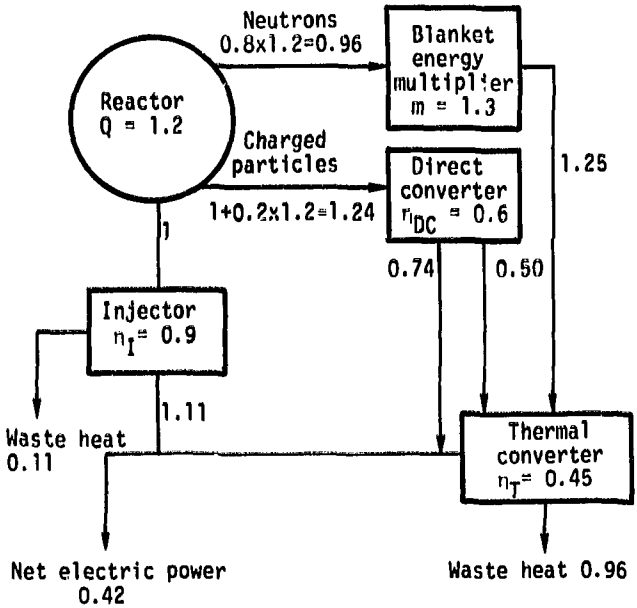

$$\eta_{sys} = \frac{0.42}{1.25+1.24-1} = 0.28$$

$$\frac{P_{net}}{P_{fus}} = \frac{0.42}{0.96+1.24-1} = 0.35$$

Fig. A-1 Reactor Power Cycle

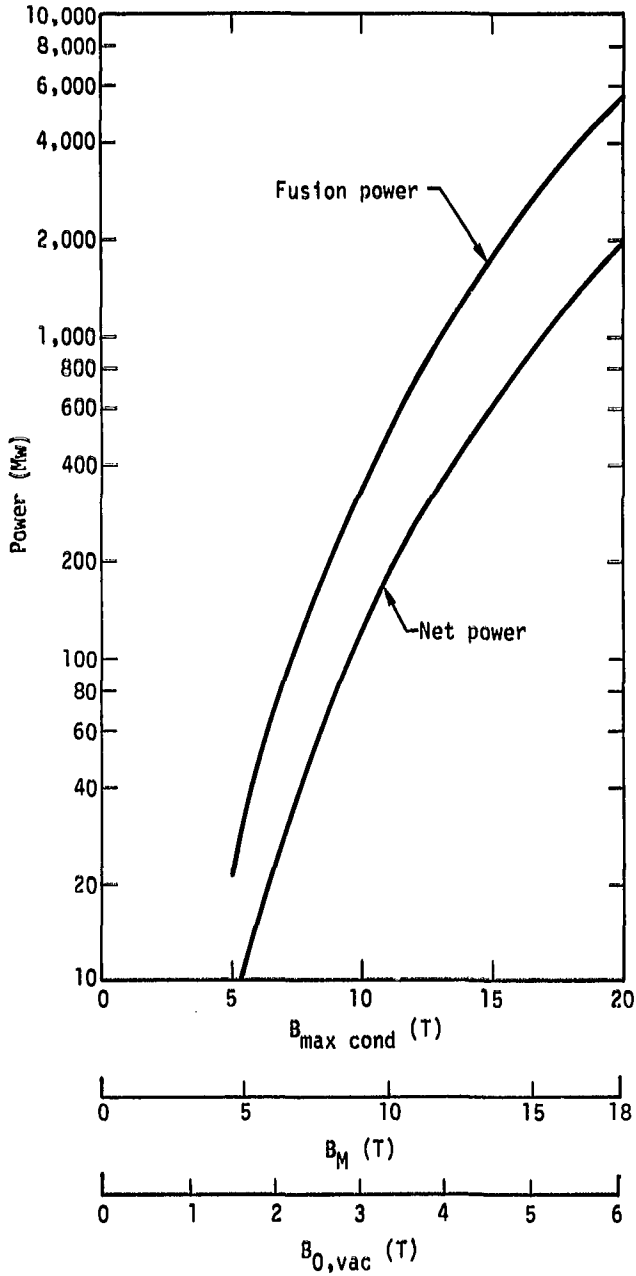

Fig. A-2 Reactor Power vs. Magnetic Field Strength

Figure B-1

Allowable Structural Envelope

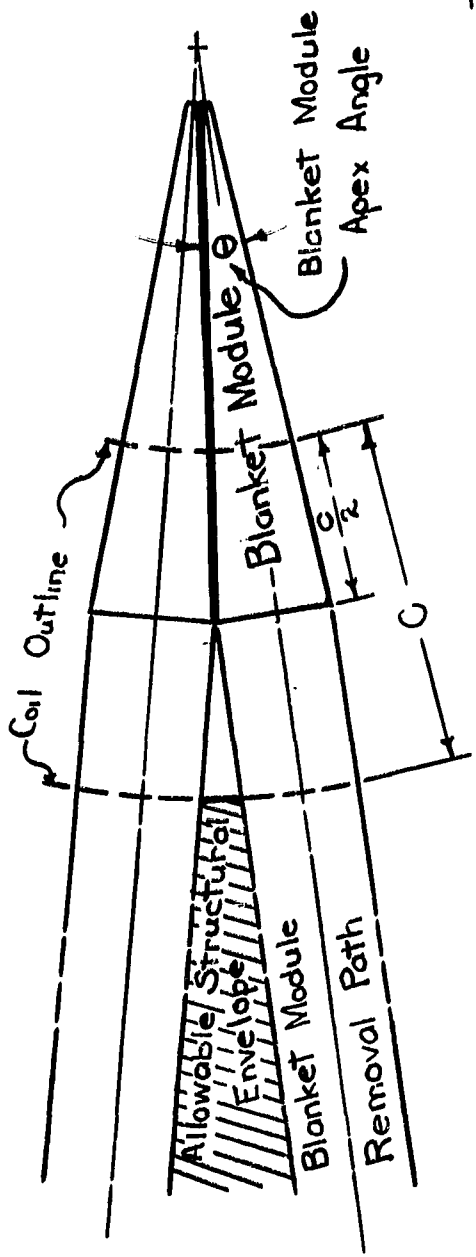

Figure B-2

Solid 'C' Clamp Structural Model

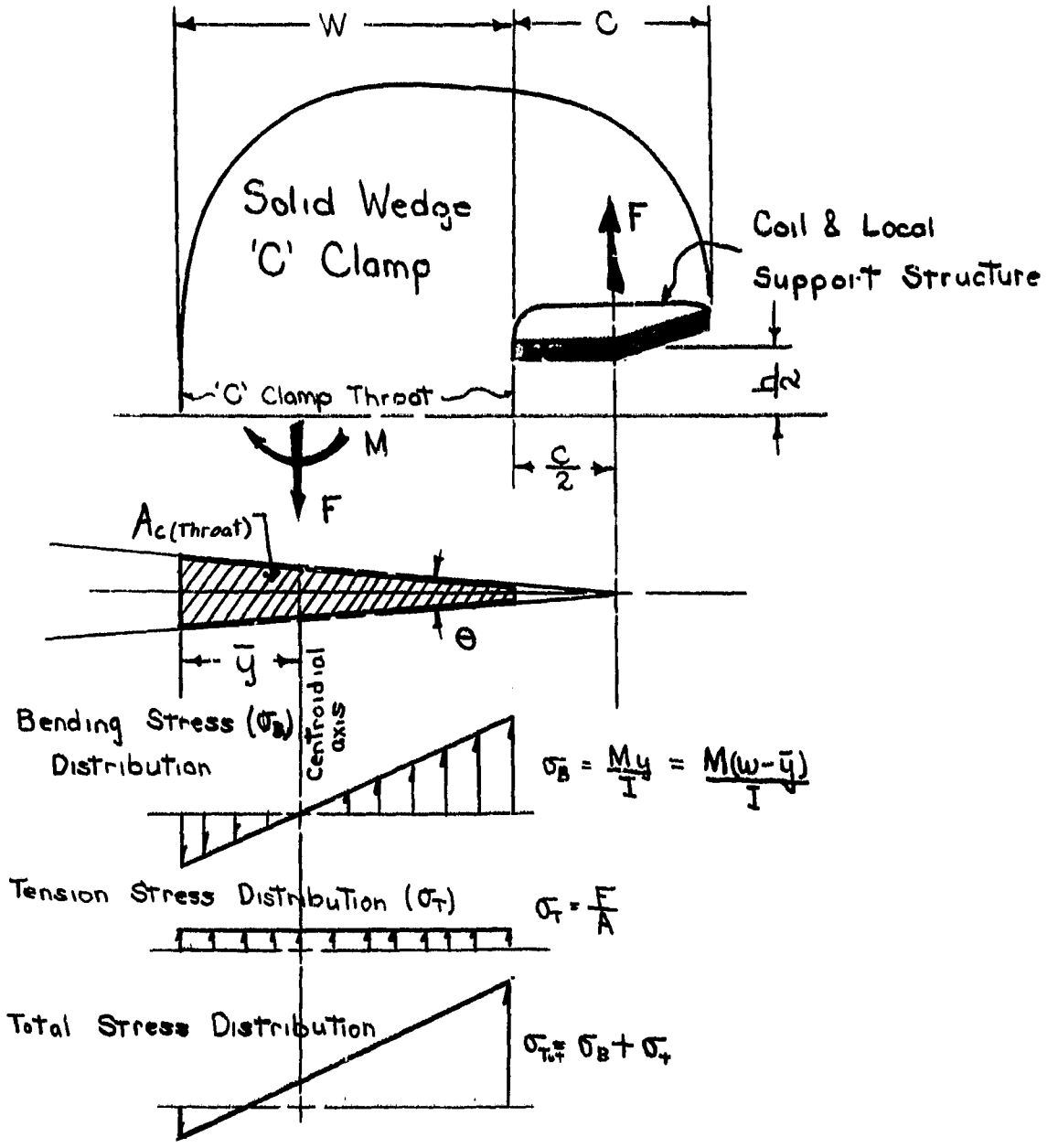

Figure B-3

Solid 'C' Clamp Volume Estimation

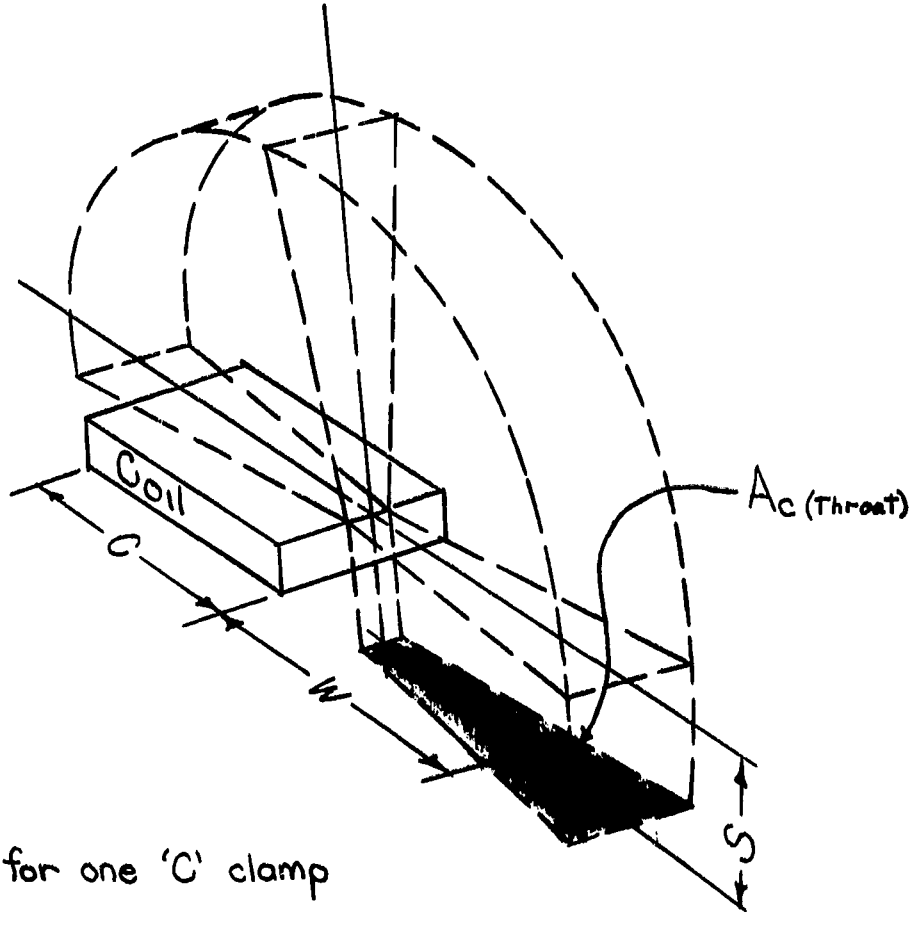

Volume for one 'C' clamp

$$V \simeq 2A_cS + 2\pi\left(\frac{C+W}{4}\right)A_c$$

Figure B-4

Truss 'C' Clamp Structure

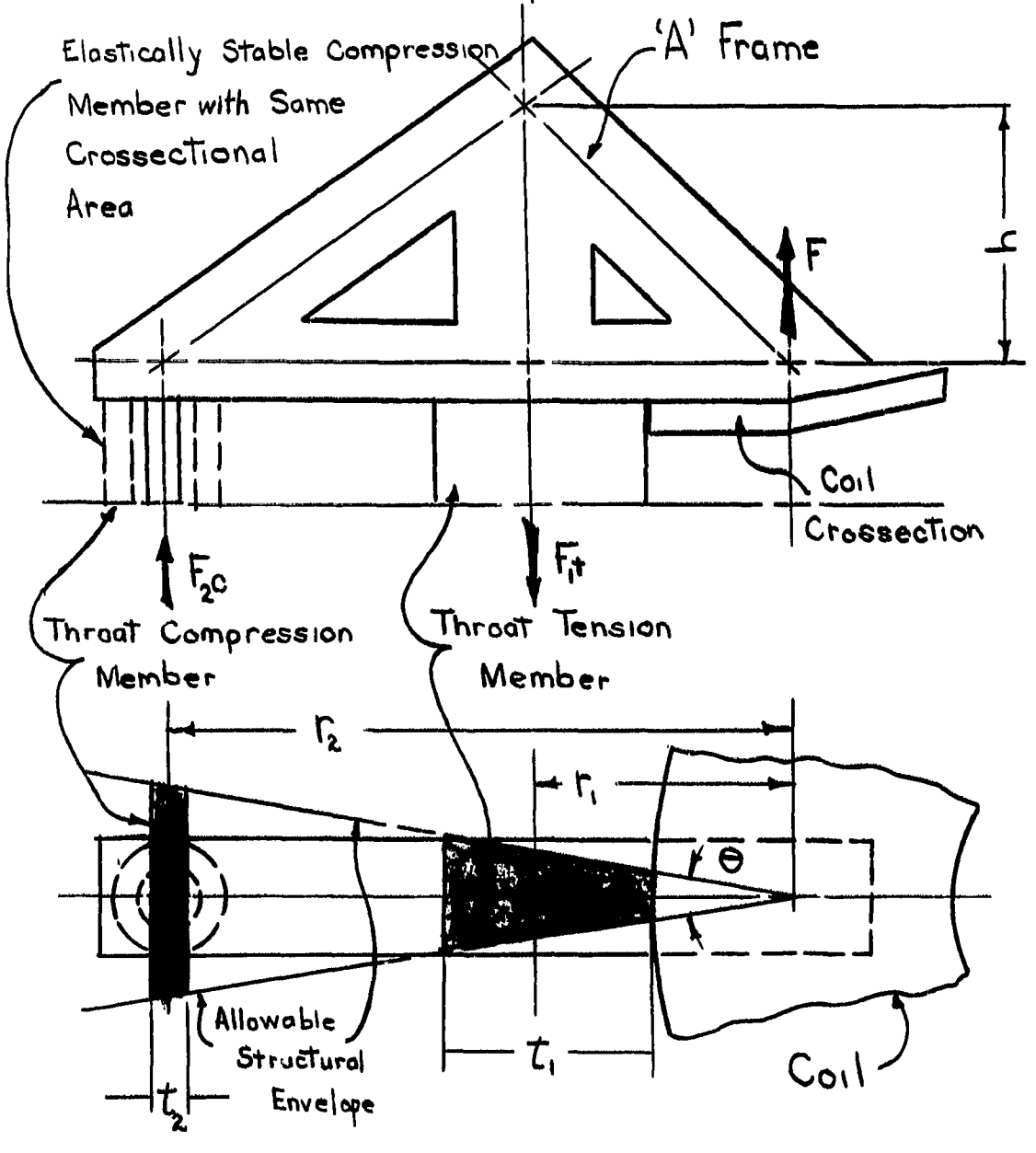

Figure B-5

Internal Coil Support Structure

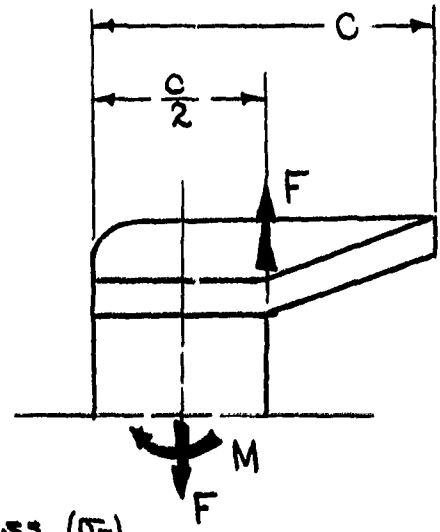

Tension Stress (σ_T)

Distribution

$\sigma_T = \frac{F}{A}$

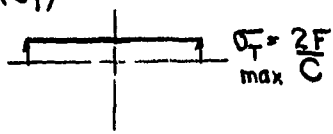

Bending Stress (σ_B)

Distribution

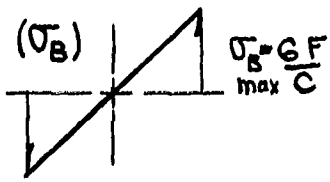

Total Stress (σ_{Tot})

Distribution

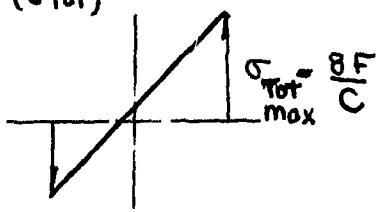

If $B_{cond} \leq 15\,T$ &

$C \leq 6.3\,m$

$\sigma_{T_{Max}} \leq 1.55 \cdot 10^8 \frac{N}{m^2}$

(22,400 psi)

$\sigma_{B_{Max}} \leq 4.64 \cdot 10^8 \frac{N}{m^2}$

(67,200 psi)

$\sigma_{Tot_{Max}} \leq 6.18 \cdot 10^8 \frac{N}{m^2}$

(89600 psi)

REFERENCES

1. Carlson, Gustav A., Selective Leakage of Charged Particles in Mirror Machines, UCRL-51434 (1973).

2. Hoffman, M. A., Werner, R. W., Heat Flux Limitations on First Wall Shields for Early Fusion Machines, UCRL-75622 (1974), also Proceedings of the First Topical Meeting on the Technology of Controlled Nuclear Fusion, AEC-Conf.-740402-P2 (1974).

3. Moir, R. W., Taylor, C. E., Magnets for Open-Ended Fusion Reactors, UCRL-74326, (1972), also Proceedings of Technology of Controlled Thermonuclear Fusion Experiments and the Engineering Aspects of Fusion Reactors, AEC-Conf.-721111 (1972).

4. Lee, J. D., Geometry and Heterogeneous Effects on the Neutronic Performance of a Yin Yang Mirror-Reactor Blanket, 5th Symposium on Engineering Problems of Fusion Research, IEEE Pub. No. 73CH0843-3NPS, p. 239, (1973).

5. R. W. Moir, "Conceptual Design Considerations for DT Mirror Reactors With and Without a Fission Blanket", UCRL-75596, also Proceedings of the First Topical Meeting on the Technology of Controlled Nuclear Fusion, AEC-Conf.-740402-P2, 1974.

6. A. H. Futch Jr., J. P. Holdren, J. Killeen, and A. A. Mirin, "Multi-Species Fokker-Planck Calculations for D-T and D-^{3}He Mirror Reactors", Plasma Physics, 14, 211, 1972.

7. R. W. Werner, G. A. Carlson, J. Hovingh, J. D. Lee and M. A. Peterson, "Progress Report #2 on the Design Considerations for a Low Power Experimental Mirror Fusion Reactor," UCRL-74054-2, 1973.

8. R. W. Moir, W. L. Barr, and G. A. Carlson, "Direct Conversion of Plasma Energy to Electricity for Mirror Fusion Reactors", UCRL-76051, also Proceedings of 5th IAEA Conf. on Plasma Physics and Controlled Nuclear Fusion Research, 1974.

9. J. Hovingh and R. W. Moir, "Efficiency of Injection of High Energy Neutral Beams into Thermonuclear Reactors," UCRL-51419, 1973.

Printed in the United States of America
Available from
National Technical Information Service
U. S. Department of Commerce
5285 Port Royal Road
Springfield, Virginia 22151
Price: Printed Copy $___*; Microfiche $2.25

*Pages	NTIS Selling Price
1-50	$4.00
51-150	$5.45
151-325	$7.60
326-500	$10.60
501-1000	$13.60